Annals of Biomedical Engineering (© 2012)
DOI: 10.1007/s10439-012-0642-0

BMES BIOMEDICAL ENGINEERING SOCIETY™ www.bmes.org

Hemodynamic Response to Repeated Noxious Cold Pressor Tests Measured by Functional Near Infrared Spectroscopy on Forehead

ZEINAB BARATI,[1] PATRICIA A. SHEWOKIS,[1,2] MELTEM IZZETOGLU,[1] ROBI POLIKAR,[3] GEORGE MYCHASKIW,[4] and KAMBIZ POURREZAEI[1]

[1]School of Biomedical Engineering, Science and Health Systems, Drexel University, 3141 Chestnut St., Bossone Research, Suite 718, Philadelphia, PA 19104, USA; [2]College of Nursing and Health Professions, Drexel University, Philadelphia, PA 19102, USA; [3]Department of Electrical and Computer Engineering, Rowan University, Glassboro, NJ 08028, USA; and [4]Department of Anesthesia, Nemours Children's Hospital, Orlando, FL 32827, USA

(*Received 3 February 2012; accepted 11 August 2012*)

Associate Editor Jane Grande-Allen oversaw the review of this article.

Abstract—The objective of this research was to assess the utility of a simple near infrared spectroscopy (NIRS) technology for objective assessment of the hemodynamic response to acute pain. For this exploration, we used functional near infrared spectroscopy (fNIRS) to measure the hemodynamic response on the forehead during three trials of a cold pressor test (CPT) in 20 adults. To measure hemodynamic changes at the superficial tissues as well as the intracranial tissues, two configurations of 'far' and 'near' source-detector separations were used. We identified two features that were found to be fairly consistent across all subjects. The first feature was the change of total hemoglobin (THb) concentration in a given condition divided by the duration of that condition THb′. Statistical analyses revealed that during the first CPT trial THb′ significantly changed from its baseline value in all channels. Also, adaptation to repeated CPTs was observed in both THb′ parameter and the reported post-stimulus pain rating scores. The second feature was the difference between the maximum and the minimum of the evoked changes in the THb concentration (ΔTHb). A significant correlation was observed between the post-stimulus pain rating score and ΔTHb at all channels. An asymmetrical activity was observed only at the 'far' channels. These results suggest that fNIRS can potentially be used as a reliable technique for the assessment of the hemodynamic response to tonic pain induced by the CPT.

Keywords—Numerical rating scale, Pain, Sympathetic nervous system.

Address correspondence to Kambiz Pourrezaei, School of Biomedical Engineering, Science and Health Systems, Drexel University, 3141 Chestnut St., Bossone Research, Suite 718, Philadelphia, PA 19104, USA. Electronic mail: kambiz@drexel.edu, kambiz.pourrezaei@drexel.edu

ABBREVIATIONS

CI	Confidence interval
CPT	Cold pressor test
CSF	Cerebrospinal fluid
FDR	False discovery rate
LED	Light emitting diode
fDA	Functional data analysis
fNIRS	Functional near infrared spectroscopy
Hb	Deoxy-hemoglobin
HbO_2	Oxy-hemoglobin
LQ	Laterality quotient
NRS	Numerical rating scale
THb	Total hemoglobin

INTRODUCTION

Cold pressor test (CPT) is a conventional test widely used in research involving psychological, cardiovascular, and neurological disorders. It was first used by Hines and Brown in 1932 to experimentally raise blood pressure for the study of hypertension.[21] The application of CPT for inducing experimental pain in healthy adults was initially introduced by Wolf and Hardy in 1941.[44] Since then, a large number of research studies have employed CPT for two main purposes: to evoke generalized sympathetic activation and to induce tonic pain.

The effect of sympathetic activation evoked by CPT on the cerebral hemodynamics has been investigated by using transcranial laser Doppler sonography for the assessment of the cerebral blood flow velocity in the middle cerebral arteries.[27,30] Sympathetically mediated changes in capillary blood flow and skin microcircula-

Published online: 07 September 2012

tion during local cooling were studied using laser Doppler flowmetry.[24] Laser Doppler utilizes low power lasers that can interrogate the outermost 0.5–1 mm depth of the skin. Single point laser Doppler systems deliver good temporal but poor spatial resolution and the measured change in blood flow greatly depends on the position of the probe relative to the location of the affected arterioles and venules.[33] Another shortcoming of single point laser Doppler is its sensitivity to motion artifacts.[33,37] Recently, laser Doppler imaging has been introduced which offers much greater spatial resolution compared to single point laser Doppler flowmetry. However, its temporal resolution is limited and the cost of the laser Doppler imaging equipment limits its routine application in clinical settings.[20]

The cortical processing of the tonic pain induced by CPT has been investigated in several neuroimaging studies. Some brain regions have been identified to be involved in the processing of noxious cold stimuli. Di Piero *et al.*[17] used a Xenon-133 inhalation single-photon emission tomography (SPET) to assess the cerebral blood flow in response to CPT performed on the left hand. They observed increased activation in regional blood flow in the contralateral frontal lobe and bilateral temporal regions as well as in the contralateral primary sensorimotor cortex in the cortical region representing the hand. In a positron emission tomography (PET) neuroimaging study, Casey *et al.*[12] found increased regional cerebral blood flow (rCBF) in response to CPT in the lateral prefrontal, anterior cingulate and insular/precentral opercular cortices ipsilaterally and in the sensorimotor cortex contralaterally.

Despite advances in imaging technology that significantly help basic science, there remains an unmet clinical need for a practical, inexpensive tool for the reliable and objective assessment of human response to pain. Recently, a few research studies suggested the use of functional near-infrared spectroscopy (fNIRS) for monitoring cortical activation in response to noxious stimuli in new-born infants,[2] healthy adults,[3,4] patients undergoing cardiac surgery,[19] and individuals suffering from migraines.[43] fNIRS is an emerging technology which enables *real time* measurement of tissue oxygenation and hemodynamics noninvasively.[31] fNIRS can be portable and has low equipment and maintenance costs. It is relatively robust to motion artifacts and therefore, no movement restriction is required during measurement, unlike the constraints imposed by other functional imaging techniques. Using the commonly used source-detector (S-D) separation distance of 2.5–4 cm, fNIRS can measure changes in blood oxygenation parameters within different layers of the head, i.e. the scalp and grey matter up to a depth of 1.25–2 cm, respectively.[25]

The main goal of the present research was to explore the potential of fNIRS for objective assessment of pain. Currently, there is no practical method available for an objective assessment of pain and clinicians are basically relying on the subjective self-report measures using limited scales. Beside the subjective nature of pain scales, their applicability for explaining different types and origins of pain is questionable. We aimed to investigate whether the hemodynamic parameters measured by fNIRS can be used as a biomarker of the tonic pain induced by CPT in healthy adults. We used a CPT as an experimental model of tonic pain because it is a conventional test that is easy to implement in experimental and clinical settings. Furthermore, healthy adults are typically familiar with the induced stimulus and the evoked response to the CPT in humans is well documented.[23,36,41]

MATERIALS AND METHODS

fNIRS Principles and Instrumentation

The fNIRS exploits the fact that in the near infrared range (700–900 nm), water, the main ingredient of tissues *in vivo*, has the lowest light absorption, whereas deoxy-hemoglobin (Hb) and oxy-hemoglobin (HbO_2) chromophores are the main absorbers with distinctive absorption characteristics.[13,22,39] By choosing two wavelengths in the near infrared spectrum and measuring the attenuation change at two different time points, the relative change in the concentration of Hb and HbO_2 molecules can be calculated using the modified Beer-Lambert law[14]

$$\Delta \mathrm{OD}_\lambda = \log\left(\frac{I_\mathrm{b}}{I_\mathrm{t}}\right) = \varepsilon_\lambda^{\mathrm{Hb}} \Delta c^{\mathrm{Hb}} \mathrm{d}\,\mathrm{DPF}_\lambda + \varepsilon_\lambda^{\mathrm{HbO_2}} \Delta c^{\mathrm{HbO_2}} \mathrm{d}\,\mathrm{DPF}_\lambda$$

where, $\Delta \mathrm{OD}_\lambda$ is termed optical density and is the change in optical intensity for the wavelength λ, I_b is the light intensity measured during baseline, I_t is the light intensity detected during or after a given task, $\varepsilon_\lambda^{\mathrm{Hb}}$ and $\varepsilon_\lambda^{\mathrm{HbO_2}}$ are the absorption coefficients of Hb and HbO_2 molecules at the wavelength λ, Δc^{Hb} and $\Delta c^{\mathrm{HbO_2}}$ are the concentration changes of Hb and HbO_2 molecules due to the task, d is the physical distance between the light source and the photodetector, and DPF_λ is the differential pathlength factor adjusted for the increased pathlength between the light source and the photodetector due to scattering at the wavelength λ. When measured at two wavelengths λ_1 and λ_2, this equation can be solved for the change in the concentration of Hb and HbO_2 molecules.

In this study, fNIRS data were collected using the continuous wave fNIRS system first described by Chance *et al.*[13] and further developed in our laboratory at Drexel University. The fNIRS system is composed of three subsystems: (1) fNIRS sensors that consist of

one light source and three photodetectors. The light source is a multi-wavelength light emitting diode (LED) manufactured by Epitex Inc. type L4*730/4*850-40Q96-I. The LED comes in a STEM TO-5 package at 730 nm and 850 nm wavelengths with an output power of 5–15 mW. The photodetectors are manufactured by Burr-Brown Corporation type OPT101 and come in an 8-pin DIP package. (2) A control box for operating the LEDs and photodetectors. (3) A computer running the COBI Studio software[1] developed in our laboratory for data acquisition and *real-time* data visualization. The fNIRS system was calibrated in our laboratory using solid and liquid phantoms with known optical absorption and scattering parameters. The detailed specification of Drexel's fNIRS system including safety assessment and signal to noise estimation are described elsewhere.[8,9,11]

The fNIRS probes used in this study utilized two configurations of S-D separation in order to test the specificity of the hemodynamic response to a CPT. Using a multi-distance probe, while the 'far' detectors sampled a superimposed hemodynamic change over a larger banana shape pathway reaching deeper layers within the head, the 'near' detector monitored the absorption changes in a shorter pathway through superficial layers, including the skin (Fig. 1). There have been several theoretical and experimental studies to detect depth-dependent changes in absorption using different S-D separations.[15,25,32]

The choice of the S-D distance in our research was made based on previous phantom experiments in our laboratory and Monte Carlo simulations by other groups. Okada *et al.*[25] reported that for an S-D separation of 15 mm and less, the mean optical path length at the deep layers is small and thus, the tissue volume being interrogated is confined to the surface layer. They also described that for an S-D spacing of 30 mm, the near infrared light penetrates into the grey matter.

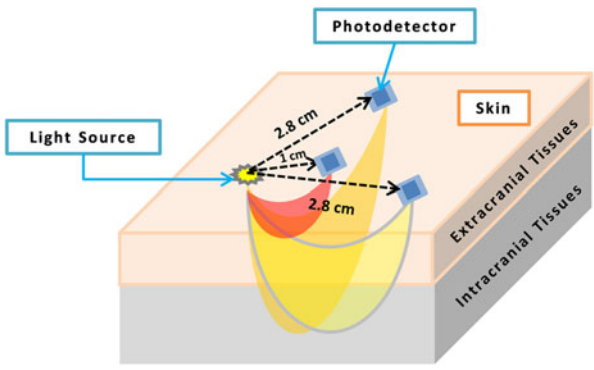

FIGURE 1. A schematic of the fNIRS probe configuration. Photons travel from a light source to a photodetector through a banana shape pathway with a penetration depth of half the source-detector distance. Measures are approximate.

In our approach in using two S-D separations to investigate the hemodynamic response at multiple layers, two detectors were placed at 2.8 cm distance from the light source (far channels), and one detector was located at 1 cm from the light source (near channel). This selection leads to a nominal penetration depth of up to 0.5 cm at the 'near channel' and up to 1.4 cm at the 'far channels' for measuring the hemodynamic changes within superficial extracranial tissues and deep intracranial layers, respectively.[34]

Subjects

Twenty healthy, right-handed, as judged by the Edinburgh Handedness Inventory[26] (Laterality Quotient (LQ): 83.03 ± 22.03), individuals (10 females) with no history of neurological, psychological, or psychiatric disorders who were analgesic-free were recruited from the Drexel University community. All participants signed the informed consent form approved by the Institutional Review Board (IRB) at Drexel University. At least 1 day prior to any experimental session, subjects were invited to participate in an orientation session in which they would perform a CPT in the real experimental setting to demonstrate the characteristics of the stimulus and to minimize anxiety associated with the initial exposure to cold water. Subjects were instructed to refrain from smoking and drinking any caffeinated or alcoholic beverages for at least 3 h before the experiment.

Protocol

Two fNIRS sensors of the same configuration as previously described were positioned symmetrically on the left and right sides of a subject's forehead proximate to the anterior median line (Fig. 2) and were secured using a medical band aid and a Velcro strap. Raw optical intensity measurements were collected at a sampling frequency of 2 Hz in a dimly lit room with an ambient temperature of ~23 °C. The effect of background light on fNIRS data was negligible and in fact, since the fNIRS measures the relative changes in Hb and HbO_2 concentrations with respect to a baseline condition, this effect was washed out in the calculations. Subjects were seated comfortably in an armchair, facing away from the experimenter to minimize any distraction.

Each experiment consisted of a baseline recording at rest followed by the immersion of the right hand up to the wrist into a bucket of circulating tepid water kept at room temperature (~23 °C) for 2 min for adaptation. Then, subjects performed three serial trials of a CPT in the ice water (~0 °C), each trial lasting 45 s followed by 2 min post-stimulus hand immersion in

the tepid water for the hemodynamic recovery. A block diagram of the protocol is shown in Fig. 3.

Both water containers were equipped with commercial aquarium pumps for water circulation to minimize heat buildup around the immersed hand.[40] The cold water container had a separate compartment for ice cubes in order to prevent any direct contact of the subject's skin with ice. Subjects received an auditory command from the experimenter when to switch their hand from the tepid water into the cold water and vice versa. At the end of each CPT and upon immersion of the hand back into the tepid water, subjects were requested to report the maximum intensity of the pain experienced during the CPT on a numerical rating scale from 0 to 10 (NRS-11), where '0' indicates no pain and '10' indicates the worst imaginable pain.[18]

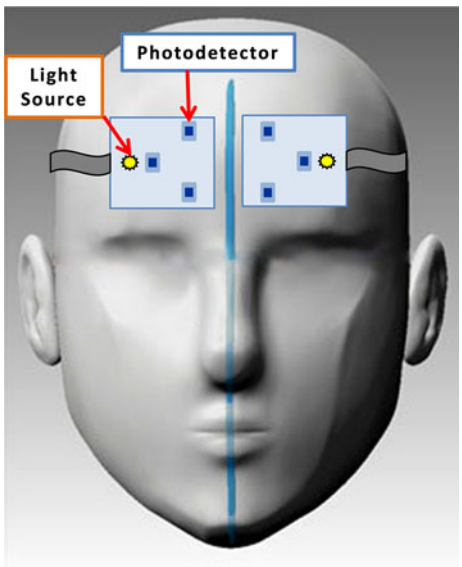

FIGURE 2. A demonstration of the placement of fNIRS probes on a subject's forehead. The probes are shown reversed to illustrate the location of the light source and photodetectors.

fNIR Data Processing

To eliminate high frequency noise, respiration and heart pulsation artifacts, raw intensity measurements were first filtered by a finite impulse response low pass filter with a cut-off frequency set to 0.14 Hz. The cut-off frequency of 0.14 Hz was determined based on our previous near infrared spectroscopy (NIRS) studies.[16]

Changes in the concentrations of Hb and HbO_2 were calculated relative to the mean value of the optical intensity during the first 15 s of the pre-stimulus baseline recording. The Hb and HbO_2 data were then smoothed using a bspline basis expansion by imposing a penalty on the roughness of the second derivative of the data with a lambda of 300.[28] Total hemoglobin (THb) concentration was obtained from:

$$\mathrm{THb} = \mathrm{Hb} + \mathrm{HbO_2}$$

All signal processing calculations were performed in MATLAB (R2011a, MathWorks, Natwick, MA) and the smoothing was performed using the functional data analysis (fDA) package for MATLAB.[28] Statistical analyses were conducted using the IBM SPSS Statistics 19. The significance criterion was $\alpha < 0.05$ for all analyses. In the case of departure from sphericity, the degree of freedom associated with the corresponding *F*-ratio was corrected using the Greenhouse–Geisser (G–G) correction value. For subjective pain ratings, a non-parametric Friedman's ANOVA by ranks with Wilcoxon Signed Ranks *post hoc* analyses were calculated. To control the type I error introduced by simultaneous testing of the experimental-wise error rate, we applied the Benjamini and Hochberg False Discovery Rate (FDR) procedure[5] to the omnibus ANOVAs and the *post hoc* multiple comparison tests.

RESULTS

The average hemodynamic response across 20 subjects is shown in Figs. 4a–4b. Here, we report the

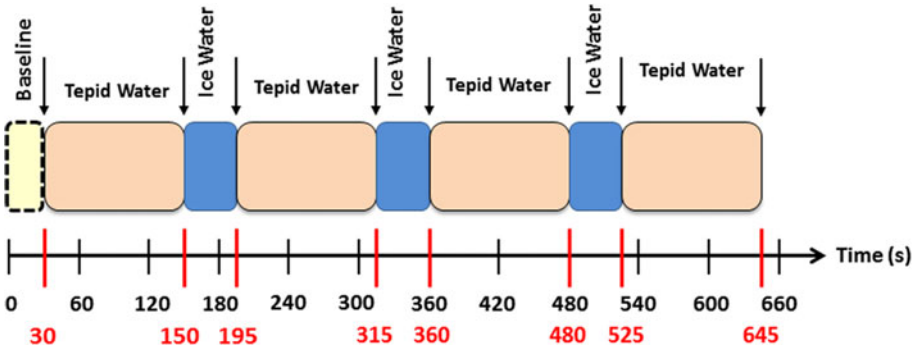

FIGURE 3. Block diagram of the protocol.

results of the analysis of THb concentration calculated as the sum of Hb and HbO_2 concentrations.

The analyses of the THb concentration were performed to assess the: (1) effect of a noxious cold water stimulus on the hemodynamic response measured by fNIRS; (2) adaptation to repeated CPTs observable in THb concentrations as well as in subjective pain scores; (3) correlation between THb concentrations and subjective pain scores within subjects; (4) specificity of the hemodynamic response to the CPTs at the superficial layers versus deep tissues; and finally (5) laterality of the hemodynamic activity measured on both sides of the forehead during the CPTs. In the following sections, we have assessed the measures and reported on our findings.

The Effect of a CPT on the THb Concentration

To assess the effect of a noxious cold water stimulus on the hemodynamic response, we compared four conditions: the initial baseline recording condition (30 s at rest), the pre-stimulus condition (the initial 2 min hand immersion in the tepid water), the first stimulus condition (the first CPT trial for 45 s) and the first post-stimulus condition (the 2 min hand immersion in the tepid water following the first CPT trial) (Fig. 5). We hypothesized that a noxious cold stimulus (ice water) would increase the blood flow to the head and consequently, the THb concentration would also increase. However, non-painful cold water (tepid water) should not change the THb concentration substantially. The dependent variable THb′ was defined as the change in THb concentration (μmoles) per a time period (in seconds) in a given condition, and was calculated by the following equation:

$$\mathrm{THb}' = \frac{(\mathrm{THb_e} - \mathrm{THb_s})|_i}{(t_e - t_s)|_i} = \frac{\Delta \mathrm{THb}_i}{\Delta t_i}$$

where, $\mathrm{THb_s}$ and $\mathrm{THb_e}$ are the values of THb concentration at the beginning and ending of a given condition, and t_s and t_e correspond to the time points where the condition begins and ends. Hence, Δt, the duration of a condition, could be 30 s, 45 s, or 2 min.

Repeated measures ANOVAs showed that THb′ significantly changed across the four conditions in all channels (Table 1). *Post hoc* FDR adjusted multiple comparisons revealed that THb′ did not significantly change from its baseline value due to hand immersion in tepid water, except for the 'near channel' on the right side of the forehead (Table 2). However, hand immersion in ice water caused a significant change in THb′ as compared to its values at both the baseline and pre-stimulus conditions and it showed a large effect ($d > 0.944$). Also, THb′ at the pre-stimulus and stimulus conditions were significantly different from their values at the post-stimulus condition which also showed large effects ($d > 1.219$).

Adaptation to Repeated CPTs Observable in Subjective Pain Ratings and THb

The adaptation to repeated trials of CPT observable in both subjective pain ratings (Fig. 6) and THb′ at the stimulus condition (Fig. 7) was further explored.

Post-stimulus pain rating scores reported based on the NRS-11 (in which '0' means no pain and '10' means the worst pain imaginable) was tested with Friedman's ANOVA by Ranks. There was a significant difference in the median value of the subjects' pain rating scores with respect to CPT trials ($\chi^2(2) = 14.70, p = 0.001$). *Post hoc* Wilcoxon signed ranks tests yielded that the intensity of the *reported* pain rating scores decreased significantly across CPT trials. It was revealed that the pain score reported after the first trial of CPT was significantly higher than the pain scores given after the second and third trials ($Z = 2.29, p = 0.02$ and $Z = 2.92, p = 0.004$, respectively). Also, the pain score reported after the second trial of CPT was significantly higher than the pain score given after the third trial ($Z = 2.59, p = 0.01$).

To assess the hemodynamic response across three CPT trials, repeated measures ANOVAs were performed on THb′ for all channels separately on the left and right sides of the forehead (Table 3). There were significant main effects of CPT trials in THb′ in all channels. FDR adjusted *post hoc* multiple comparisons showed that THb′ at the first CPT trial was significantly different from the THb′ at the second and third CPT trials in all channels on both sides of the forehead with large effects ($d > 0.886$) (Table 4, Fig. 8). However, except for the 'near channel' on the left side, THb′ values at the second and third CPT trials were not significantly different. This significant difference represented a moderate effect ($d = 0.573$).

We experimentally identified another feature which may be a better representation of the individualized hemodynamic response to CPTs. This variable, which is denoted as ΔTHb, is expected to account for the inter-subject variability in the latency of the hemodynamic response and is defined as the change in the THb concentration induced by each CPT. ΔTHb is calculated as the difference between the minimum value of THb that is obtained within 20 s after hand immersion in ice water and the maximum value of THb within a 35 s window starting 15 s before removing the hand from the ice water and ending 20 s after it (Figs. 9a–9c). The minimum value of THb was searched within a region when the effect of CPT is expected to be minimal. The maximum value of THb was searched within a

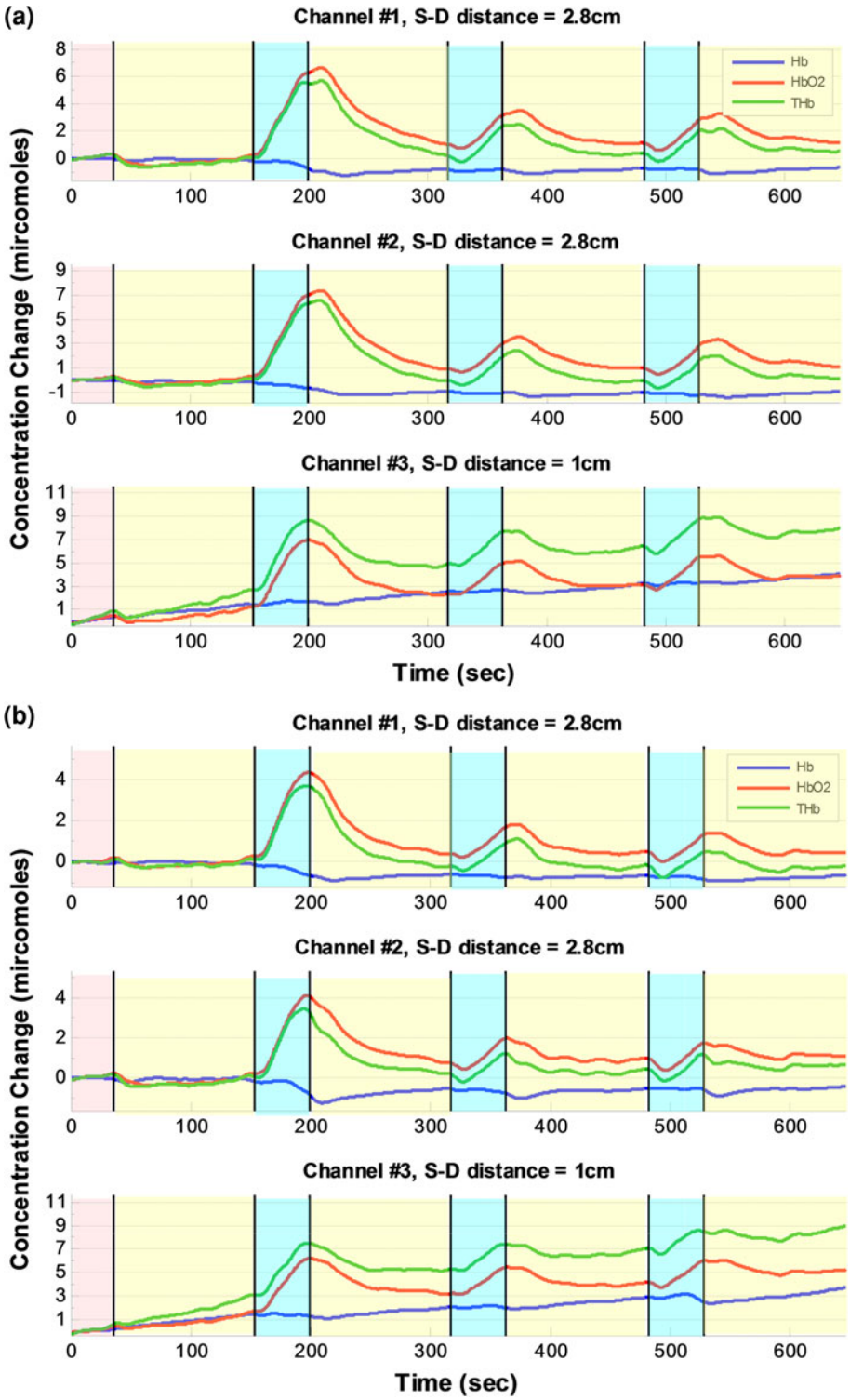

FIGURE 4. (a–b) The hemodynamic response to three trials of cold pressor test (CPT) averaged across 20 subjects on the right (a) and left (b) sides of the forehead. The black vertical lines represent time points at which subjects switched their hand from the tepid water to the ice water and vice versa. The pink shaded field represents the baseline period, the orange shaded fields represent the immersion in tepid water condition, and the blue shaded fields represent the CPT conditions. Hb, HbO_2 and THb are abbreviations for deoxy-hemoglobin, oxy-hemoglobin and total hemoglobin, respectively. 'S-D' symbol stands for 'source-detector'.

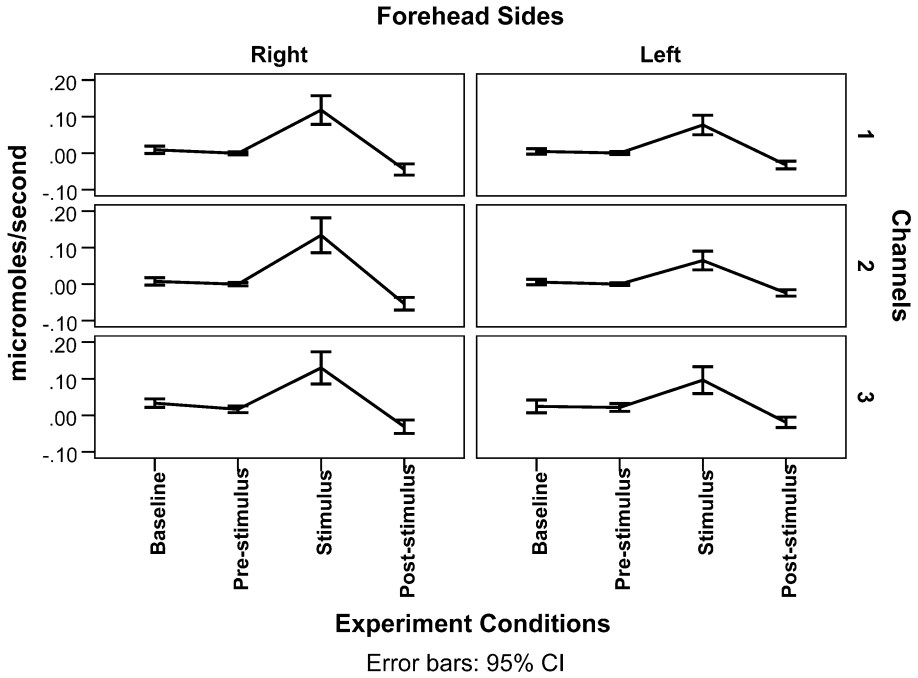

FIGURE 5. Line graphs of THb′ during four experimental conditions: baseline, pre-stimulus, stimulus, and post-stimulus conditions (for the definition of THb′, please see "The Effect of a CPT on the THb Concentration" section). Error bars represent the 95% confidence intervals (CI).

TABLE 1. Results of repeated measures ANOVA on THb′ during the four experimental conditions: baseline, pre-stimulus, stimulus, and post-stimulus conditions.

		THb′ (μmoles/s)(mean ± SD[a])				
Forehead side	Channel	Baseline	Pre-stimulus	Stimulus	Post-stimulus	Repeated measures ANOVA*
Right	1 (2.8 cm)	0.00 ± 0.02	−0.00 ± 0.01	0.12 ± 0.08	−0.05 ± 0.03	$F(1.12, 21.29) = 37.16$ G–G[b] $p < 0.001$
	2 (2.8 cm)	0.01 ± 0.02	−0.00 ± 0.01	0.13 ± 0.10	−0.05 ± 0.04	$F(1.08, 20.49) = 33.71$ G–G $p < 0.001$
	3 (1 cm)	0.03 ± 0.03	0.02 ± 0.02	0.13 ± 0.09	−0.03 ± 0.04	$F(1.10, 20.01) = 29.54$ G–G $p < 0.001$
Left	1 (2.8 cm)	0.00 ± 0.02	0.00 ± 0.01	0.08 ± 0.06	−0.03 ± 0.02	$F(1.14, 21.65) = 35.16$ G–G $p < 0.001$
	2 (2.8 cm)	0.01 ± 0.02	−0.00 ± 0.01	0.06 ± 0.05	−0.02 ± 0.02	$F(1.13,21.38) = 25.50$ G–G $p < 0.001$
	3 (1 cm)	0.02 ± 0.04	0.02 ± 0.02	0.10 ± 0.08	−0.02 ± 0.03	$F(1.29,24.56) = 25.66$ G–G $p < 0.001$

* Experiment-wise error rates are False Detection Rate (FDR) adjusted (p values).
[a]'SD' stands for 'standard deviation'.
[b]Due to departure from sphericity, the degrees of freedom were adjusted using the Greenhouse–Geisser (G–G) correction value.

window in which the cumulative effect of CPT was expected to reach its maximum with enough time for the hemodynamics to fully evolve. Although we acknowledge that within the selected time windows subjects may be cognitively involved in anticipating the next stimulus or reporting their pain, the effect of these cognitive tasks on the hemodynamics is considered to be much lower than the observed effect of a cold water stimulus and thus, it can be disregarded.

Correlation Analysis Between ΔTHb and Subjective Pain Scores

A secondary interest was to determine whether a decrease in the reported pain scores across the three CPT trials within a subject was associated with a decrease in the measured hemodynamic parameter (i.e. ΔTHb). To answer this question, within-subjects correlation coefficients[6] were calculated. All the correlation values were significant at the 0.05 level and

TABLE 2. Pairwise condition comparisons across the Forehead Side and Channel including 95% confidence intervals and effect sizes for THb′, comparing the four conditions: the baseline, 1st pre-stimulus, 1st stimulus, and 1st post-stimulus conditions.

			95% CI[a] of the difference			
Forehead side	Channel	Pairs of conditions	Lower limit	Upper limit	*p* value*	Cohen's d
Right	1 (2.8 cm)	Baseline—pre-stimulus	−0.001	0.020	0.075	–
		Baseline—stimulus	**−0.150**	**−0.067**	**00.001**	**1.222**
		Baseline—post-stimulus	**0.038**	**0.070**	**<0.001**	**1.563**
		Pre-stimulus—stimulus	**−0.158**	**−0.079**	**<0.001**	**1.414**
		Pre-stimulus—post-stimulus	**0.028**	**0.060**	**<0.001**	**1.276**
		Stimulus—post-stimulus	**0.109**	**0.216**	**<0.001**	**1.429**
	2 (2.8 cm)	Baseline—pre-stimulus	−0.002	0.017	0.110	–
		Baseline—stimulus	**−0.178**	**−0.075**	**<0.001**	**1.149**
		Baseline—post-stimulus	**0.043**	**0.079**	**<0.001**	**1.584**
		Pre-stimulus—stimulus	**−0.182**	**−0.086**	**<0.001**	**1.318**
		Pre-stimulus—post-stimulus	**0.035**	**0.072**	**<0.001**	**1.359**
		Stimulus—post-stimulus	**0.123**	**0.252**	**<0.001**	**1.359**
	3 (1 cm)	Baseline—pre-stimulus	**0.008**	**0.026**	**0.001**	**0.871**
		Baseline—stimulus	**−0.140**	**−0.053**	**<0.001**	**1.031**
		Baseline—post-stimulus	**0.045**	**0.084**	**<0.001**	**1.555**
		Pre-stimulus—stimulus	**−0.153**	**−0.068**	**<0.001**	**1.184**
		Pre-stimulus—post-stimulus	**0.031**	**0.064**	**<0.001**	**1.351**
		Stimulus—post-stimulus	**0.102**	**0.220**	**<0.001**	**1.280**
Left	1 (2.8 cm)	Baseline—pre-stimulus	−0.003	0.013	0.229	–
		Baseline—stimulus	**−0.101**	**−0.044**	**<0.001**	**1.183**
		Baseline—post-stimulus	**0.026**	**0.048**	**<0.001**	**1.568**
		Pre-stimulus—stimulus	**−0.105**	**−0.049**	**<0.001**	**1.279**
		Pre-stimulus—post-stimulus	**0.023**	**0.042**	**<0.001**	**1.570**
		Stimulus—post-stimulus	**0.073**	**0.145**	**<0.001**	**1.422**
	2 (2.8 cm)	Baseline—pre-stimulus	−0.002	0.014	0.129	–
		Baseline—stimulus	**−0.088**	**−0.030**	**<0.001**	**0.944**
		Baseline—post-stimulus	**0.021**	**0.038**	**<0.001**	**1.687**
		Pre-stimulus—stimulus	**−0.091**	**−0.038**	**<0.001**	**1.136**
		Pre-stimulus—post-stimulus	**0.015**	**0.033**	**<0.001**	**1.219**
		Stimulus—post-stimulus	**0.055**	**0.122**	**<0.001**	**1.225**
	3 (1 cm)	Baseline—pre-stimulus	−0.010	0.016	0.640	–
		Baseline—stimulus	**−0.107**	**−0.037**	**<0.001**	**0.967**
		Baseline—post-stimulus	**0.027**	**0.060**	**<0.001**	**1.236**
		Pre-stimulus—stimulus	**−0.110**	**−0.040**	**<0.001**	**0.999**
		Pre-stimulus—post-stimulus	**0.030**	**0.052**	**<0.001**	**1.759**
		Stimulus—post-stimulus	**0.074**	**0.157**	**<0.001**	**1.298**

*Significant results (False Detection Rate (FDR) adjusted) are shown in bold.
[a]'CI' stands for 'confidence interval'.

showed a moderate to large effects (ranging from 0.50 to 0.67), corresponding to a linear relation between the subjective pain rating scores and ΔTHb within subjects (Table 5).

Comparing ΔTHb Response at the 'Far Channels' with the 'Near Channels' Across Left and Right Sides of the Forehead

Separate 2 × 3 (Forehead Side by Channel) repeated measures ANOVAs on ΔTHb were performed for each CPT trial to assess the laterality and specificity of the hemodynamic activity. Specificity of the hemodynamic response was measured by 'far channels 1 and 2' representing the intracranial layers and a 'near channel' representing the superficial tissues. Greenhouse–Geisser (G–G) corrections were applied for violations of the sphericity assumption on the repeated measures tests.

Results of the 2 × 3 (Forehead Side by Channel) repeated measures ANOVAs on ΔTHb showed significant interactions between the Forehead Side and Channel for every three CPT trials ($F(2.26, 42.95) = 5.78$ G–G, $p = 0.004$, $F(3.05,58.03) = 5.46$ G–G, $p = 0.002$, $F(2.18,41.33) = 7.37$ G–G, $p = 0.001$; for the first, second and third CPT trials, respectively). There was a significant main effect of the Forehead Side for all CPT trials ($F(1,19) = 8.69$, $p = 0.008$, $F(1,19) = 8.40$, $p = 0.009$, $F(1,19) = 8.04$, $p = 0.01$; for the first, second and third CPT trials, respectively)

and a significant main effect of the Channel for the second and third CPT trials ($F(2,38) = 4.70$ G–G, $p = 0.02$, $F(2,38) = 10.75$, $p < 0.001$) (Fig. 10).

Post hoc multiple comparisons after controlling the FDR showed that there is no significant difference between the 'near channel' and 'far channels' on either side of the forehead.

Significant asymmetrical activity was revealed by the FDR adjusted *post hoc* tests on the ΔTHb response measured by the 'far channels', indicating moderate-to-large effects ($0.697 \leq d \leq 0.902$). However, there was no laterality in the ΔTHb for the superficial tissues as measured by the 'near channels' (Table 6).

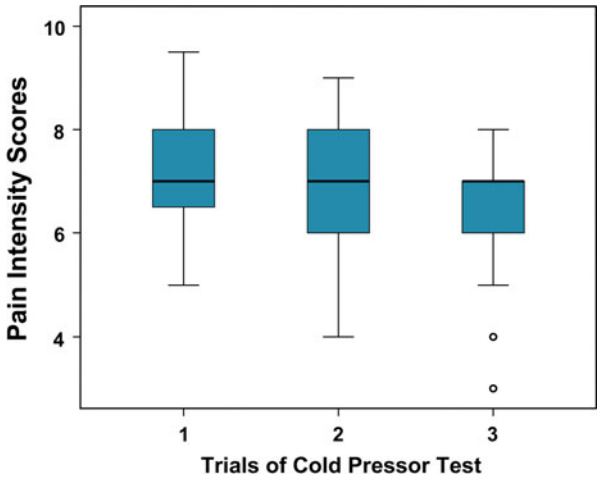

FIGURE 6. Boxplots of post-stimulus pain rating scores of 20 subjects across three trials of cold pressor test (CPT). Two outliers were identified for pain scores reported after 3rd trial of CPT and are represented as circles.

DISCUSSION

Despite the technological advancement in medical device development, effective assessment and management of pain is poorly addressed. One possible reason could be the subjectivity of the pain experience. It is well know that the pain experience including its perception and expression is highly individualized. Therefore, there is a need for a more objective assessment of pain.

In the conventional pain practice, vital signs such as heart rate, blood pressure, respiratory rate, galvanic skin response and/or cutaneous blood flow measured by laser Doppler flowmetry have been used to monitor the physiological parameters in response to a noxious stimulus. However, the clinical experience has proven that these physiological signs are not practically reliable and should be interpreted cautiously. For instance, physiological parameters change due to many factors other than pain such as distress, medications, and illness. Laser Doppler flowmetry data are also very noisy and the smallest motion causing any change in the contact between the probe tip and the skin creates a drastic change in the signal. Further, since the typical depth of penetration for a laser Doppler flowmeter is

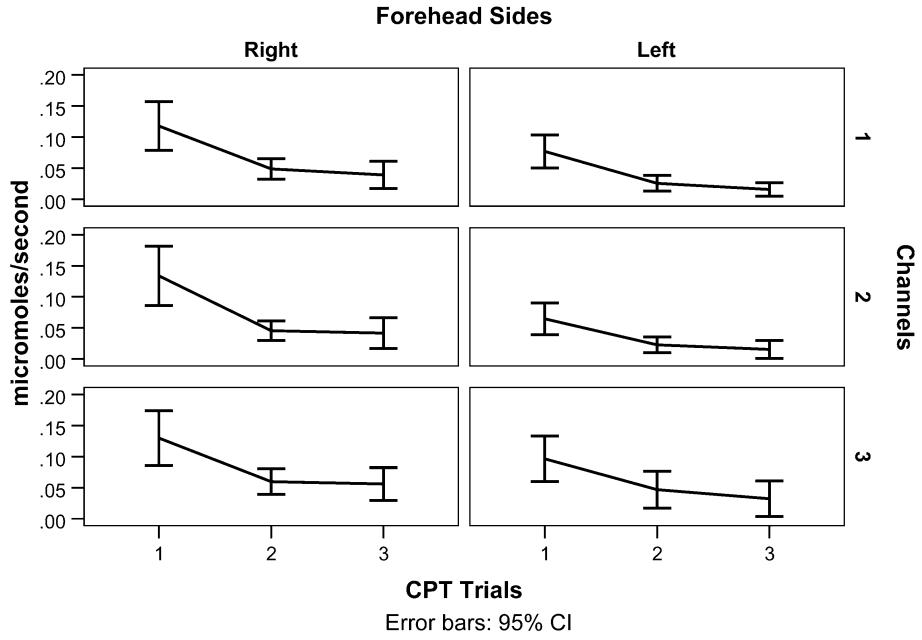

FIGURE 7. Line graphs of THb′ across cold pressor test (CPT) trials (for the definition of THb′, please see "The Effect of a CPT on the THb Concentration" section).

TABLE 3. Main effect of cold pressor test (CPT) trials repeated measures ANOVAs on THb′.

		THb′ (μmoles/s)(mean ± SD[a])			
Forehead Side	Channel	1st CPT	2nd CPT	3rd CPT	Repeated Measures ANOVA*
Right	1 (2.8 cm)	0.12 ± 0.08	0.05 ± 0.04	0.04 ± 0.05	$F(1.38,26.20) = 31.41$ G–G[b] $p < 0.001$
	2 (2.8 cm)	0.13 ± 0.10	0.05 ± 0.03	0.04 ± 0.05	$F(1.32,25.08) = 27.27$ G–G $p < 0.001$
	3 (1 cm)	0.13 ± 0.09	0.06 ± 0.04	0.06 ± 0.06	$F(1.49,28,35) = 16.83$ G–G $p < 0.001$
Left	1 (2.8 cm)	0.08 ± 0.06	0.03 ± 0.03	0.02 ± 0.02	$F(1.32,25.03) = 24.62$ G–G $p < 0.001$
	2 (2.8 cm)	0.06 ± 0.05	0.02 ± 0.03	0.02 ± 0.03	$F(1.44,27.30) = 23.18$ G–G $p < 0.001$
	3 (1 cm)	0.10 ± 0.08	0.05 ± 0.06	0.03 ± 0.06	$F(1.55,29.36) = 32.20$ G–G $p < 0.001$

*Experiment-wise error rates are False Detection Rate (FDR) adjusted (p values).
[a]'SD' stands for 'standard deviation'.
[b]Due to departure from sphericity, the degrees of freedom were adjusted using the Greenhouse–Geisser (G–G) correction value.

TABLE 4. Pairwise cold pressor test (CPT) trials comparisons across the Forehead Side and Channel including 95% confidence intervals and effect sizes for THb′.

			95% CI[a] of the difference			
Forehead Side	Channel	Pair of CPT	Lower Limit	Upper Limit	p-value*	Cohen's d
Right	1 (2.8 cm)	1st CPT—2nd CPT	**0.043**	**0.095**	**<0.001**	**1.266**
		1st CPT—3rd CPT	**0.052**	**0.106**	**<0.001**	**1.376**
		2nd CPT—3rd CPT	−0.003	0.023	0.138	–
	2 (2.8 cm)	1st CPT—2nd CPT	**0.051**	**0.125**	**< 0.001**	**1.117**
		1st CPT—3rd CPT	**0.061**	**0.123**	**< 0.001**	**1.391**
		2nd CPT—3rd CPT	−0.013	0.021	0.637	–
	3 (1 cm)	1st CPT—2nd CPT	**0.033**	**0.107**	**0.001**	**0.886**
		1st CPT—3rd CPT	**0.045**	**0.103**	**<0.001**	**1.184**
		2nd CPT—3rd CPT	−0.018	0.025	0.726	–
Left	1 (2.8 cm)	1st CPT—2nd CPT	**0.027**	**0.076**	**<0.001**	**0.964**
		1st CPT—3rd CPT	**0.041**	**0.082**	**<0.001**	**1.389**
		2nd CPT—3rd CPT	−0.002	0.021	0.088	–
	2 (2.8 cm)	1st CPT—2nd CPT	**0.022**	**0.062**	**<0.001**	**0.971**
		1st CPT—3rd CPT	**0.033**	**0.066**	**<0.001**	**1.392**
		2nd CPT—3rd CPT	−0.004	0.18	0.174	–
	3 (1 cm)	1st CPT—2nd CPT	**0.029**	**0.070**	**<0.001**	**1.131**
		1st CPT—3rd CPT	**0.045**	**0.083**	**<0.001**	**1.588**
		2nd CPT—3rd CPT	**0.003**	**0.027**	**0.020**	**0.573**

*Significant results (after controlling the False Detection Rate (FDR)) are shown in bold.
[a]'CI' stands for 'confidence interval'.

less than 1 mm, the results are very sensitive to the type of the skin and the location where the probing is conducted.[33,37]

Over the past 5 years, we have used fNIRS for monitoring hemodynamic response to noxious stimuli. We aimed to find an association between a noxious stimulus and the evoked hemodynamic response and to demonstrate that induced noxious stimuli elicit a reproducible and consistent hemodynamic response which can be reliably detected by fNIRS. During this period, we have explored different protocols by changing the setting of the stimulus such as type, intensity and duration as well as fNIRS probe configurations in an effort to optimize the reproducibility and strength of the response. The results presented in this manuscript demonstrate only a piece of our quest to identify reliable and robust stimulus–response parameters. The present study aimed to investigate the hemodynamic changes during repeated CPTs employed as an experimental model of the tonic pain

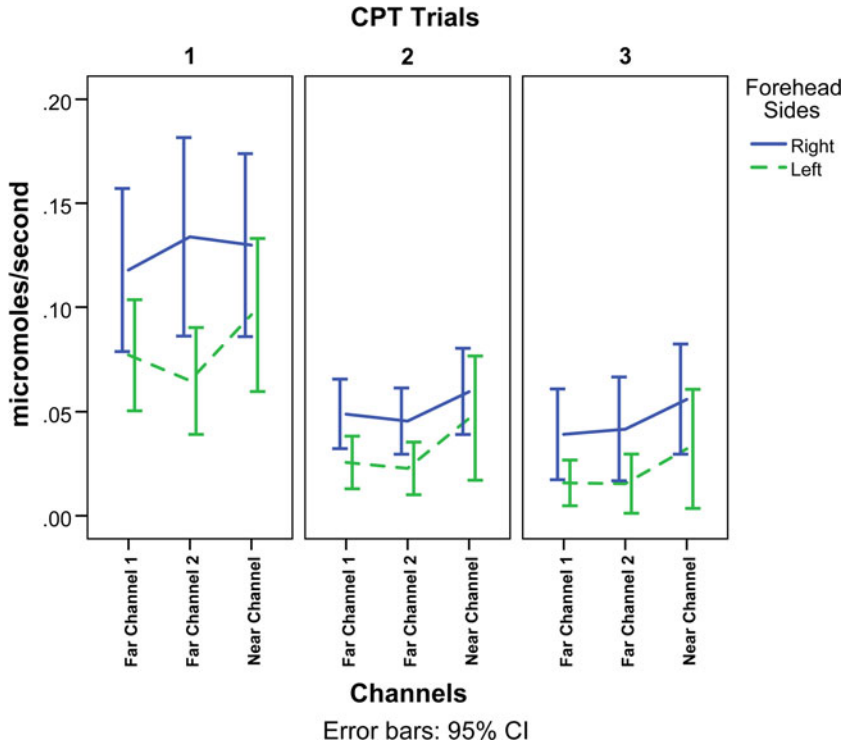

FIGURE 8. Line graphs of THb′ for separate trials of cold pressor test (CPT) (for the definition of THb′, please see "The Effect of a CPT on the THb Concentration" section). Significant interactions between the Forehead Side and Channel were found for the 1st and 2nd CPT trials.

with the capability of evoking a general acute sympathetic activation. We established that a simple NIRS device can effectively monitor the hemodynamic response to a CPT. Since the signal penetrates deeper and the light source and detector are directly in contact with the skin, there is a negligible noise due to the movement of components with respect to the skin.

According to the literature, cold sensation, at freezing temperatures, becomes painful within the initial 10 s and progressively increases until it reaches its maximum at approximately 60 s.[41] Based on our pilot experiments, we observed that 45 s was a reasonable duration of a CPT to induce an acute pain response in normal subjects and also to allow a detectable hemodynamic response to evolve. Moreover, the 2 min post-stimulus immersion in the tepid water was sufficient time for the hemodynamic response to get close to a steady state. In retrospect, we realized that we could have allowed more time between CPTs to let the hemodynamics return to its initial baseline level. However, we tried to keep the duration of the experiment as brief as possible to avoid our subjects becoming bored and other potential confounds.

It is suggested that for a stimulus that lasts for 1 s, the hemodynamic response evolves over 10–12 s with some components having longer recovery time.[10] For longer events, the hemodynamic response adds up roughly linearly over time.[7] The selected search windows for calculating the ΔTHb were determined experimentally using our small sample size. We noticed that some subjects reached their maximum THb value as soon as 30 s after starting a CPT. Consequently, we chose to extend the search window for the maximum THb response to 15 s before the termination of the CPT and 20 s after it in all trials.

The tonic pain induced by noxious cold water is massively confounded and regulated by sympathetic activity. Thus, it is plausible to conclude that the observed hemodynamic change in response to CPT is mainly dominated by the sympathetic nervous system in terms of global increase in cerebral blood flow as a consequence of the increase in cardiac output following painful stimuli. The observed asymmetric change in ΔTHb at the intracranial tissues as measured by the 'far channels' and no laterality in the superficial tissues as measured by the 'near channels' could be indicators of the presence of simultaneous activations of the systemic sympathetic system as well as higher cerebral regulatory systems. While the results of this study are consistent with the previously reported cerebral asymmetry in regulations of the autonomic nervous system,[38] further investigations are required prior to making any conclusion on the hemisphere specificity in response to a CPT.

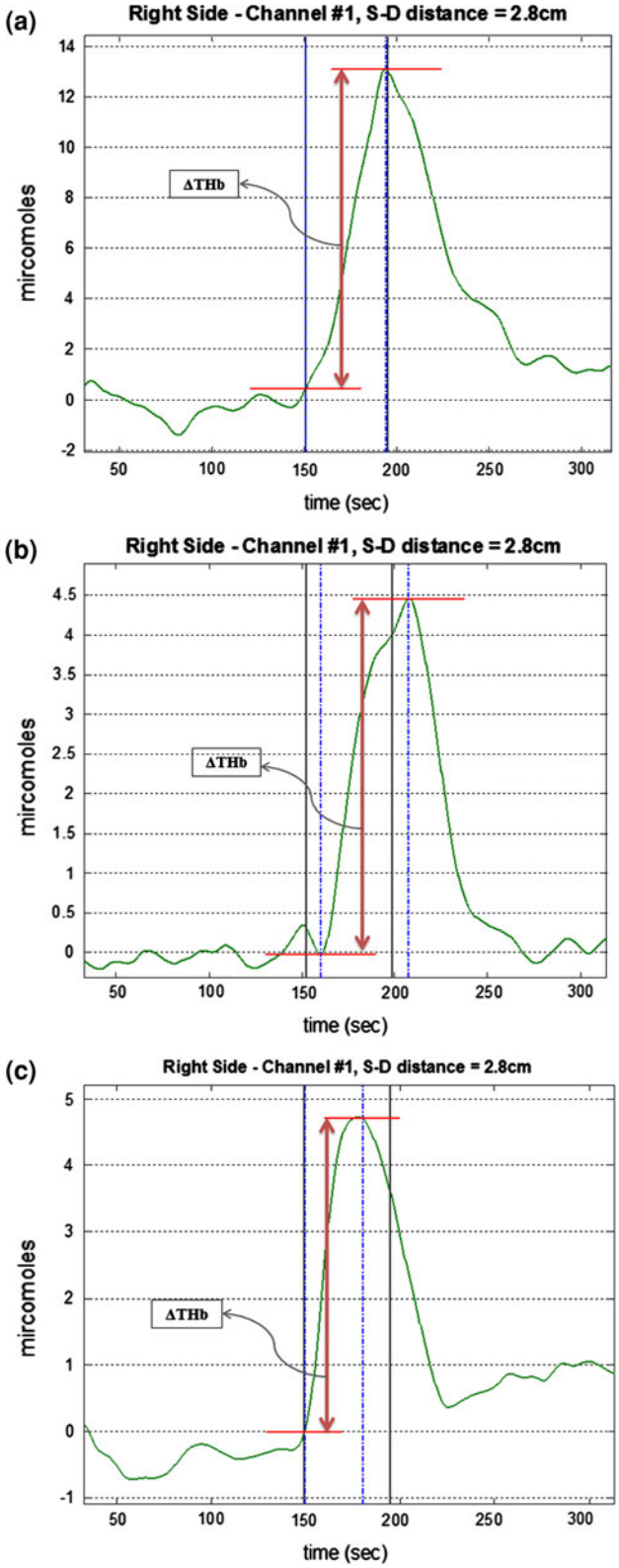

FIGURE 9. (a–c) Three sample total hemodynamic responses to the first cold pressor test (CPT) measured at the 'far channel 1' on the right side of the forehead. The first black vertical line represents the time point at which subjects immersed their hand into the ice water and the second black vertical line shows the time when subjects immersed their hand back into the tepid water. Dashed blue vertical lines represent the detected time points for ΔTHb calculation (see ''Correlation Analysis between ΔTHb and Subjective Pain Scores'' section).

Our experimental results did not provide any strong evidence to link the observed lateralized activation in the prefrontal region to any specific pain-induced cortical activity; partly due to the type of the stimulus applied and limited data analyses techniques used. However, a NIRS study suggests that a stress-inducing mental task induces asymmetrical activities in the prefrontal cortex.[38] Thus, the lateralized activation in the prefrontal region could be related in part to the stress induced by a CPT or may reflect a general arousal due to a cold water stimulus.

Repeated CPTs have been previously used to investigate cardiovascular habituation and to activate endogenous analgesic systems.[35,42] In the present study, three trials of CPT were performed to test the reliability of our measurements as well as to study the adaptation in our sample regarding subjective pain scores and the objective hemodynamic measurements. We observed that THb′ responses had significantly different values in the second and third CPT trials as compared to the first CPT trial in all channels with large effect sizes ($d > 0.886$). However, no significant difference was found between the THb′ in the second and third CPT trials, except for one channel (the 'near channel' on the left side of the forehead). This observation suggests that the hemodynamic activity adapts to repeated trials of CPT. Furthermore, the median of pain rating scores, which is a subjective measure, also decreased across the CPT trials as a manifestation of the subjects' adaptation to the pain. The correlation analysis showed a moderate to large effect size corresponding to a strong association between the ΔTHb and pain rating scores within subjects. However, a future study that benefits from a significantly larger sample size needs to be conducted to further validate this association. Since self-reporting is very subjective in nature, an absolute correlation between fNIRS parameters and self-reported pain

TABLE 5. Within-subjects correlation values between self-reported pain rating scores and ΔTHb.

Forehead Side	Channel	Within-subjects correlation*
Right	Far channel 1	0.609
	Far channel 2	0.577
	Near channel	0.541
Left	Far channel 1	0.556
	Far channel 2	0.495
	Near channel	0.670

*All the correlation coefficients were significant at a 0.05 level.

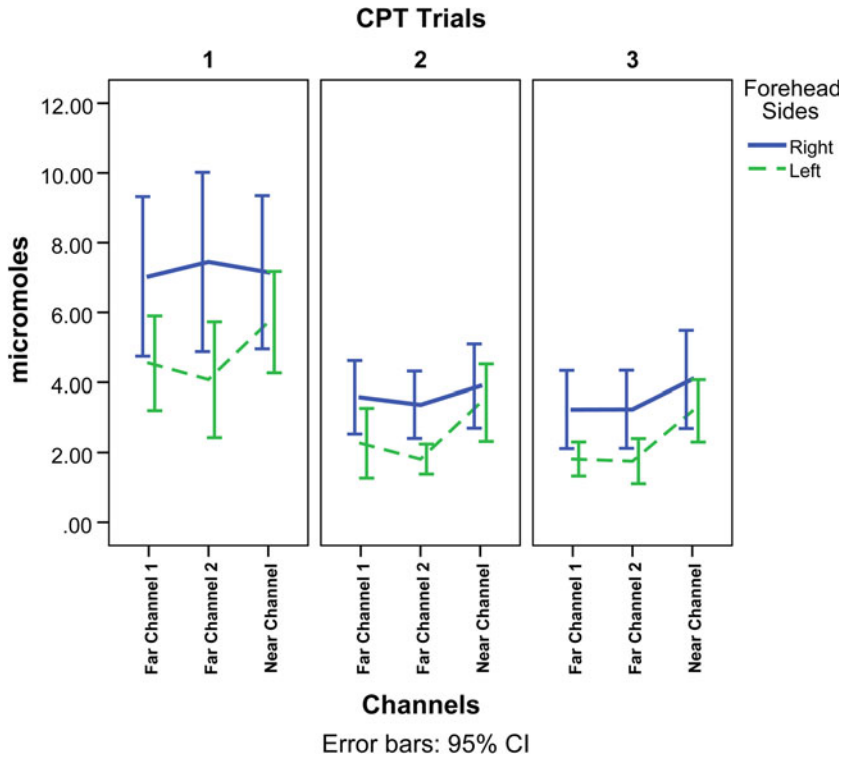

FIGURE 10. Line graphs of ΔTHb for separate trials of cold pressor test (CPT) (for the definition of ΔTHb, please see Figs. 9a–9c). For all three trials of CPT, significantly different activation on the left and right sides of the forehead was observed in ΔTHb as measured by the 'far channels', while no laterality was observed in ΔTHb as measured by the 'near channels'.

TABLE 6. Pairwise channel pair comparisons across cold pressor test (CPT) trials including 95% confidence intervals and effect sizes for ΔTHb.

CPT trial	Pair of channels	95% CI[a] of the difference		*p*-value*	Cohen's d
		Lower limit	Upper limit		
1st	Right far channel 1—left far channel 1	**0.817**	**4.151**	**0.006**	**0.697**
	Right Far channel 2—left far channel 2	**1.513**	**5.225**	**0.001**	**0.849**
	Right near channel—left near channel	−0.793	3.652	0.194	–
2nd	Right far channel 1—left far channel 1	**0.595**	**2.025**	**0.001**	**0.857**
	Right far channel 2—left far channel 2	**0.619**	**2.483**	**0.002**	**0.779**
	Right near channel—left near channel	−0.866	1.818	0.467	–
3rd	Right far channel 1—left far channel 1	**0.614**	**2.214**	**0.002**	**0.827**
	Right far channel 2—left far channel 2	**0.713**	**2.251**	**0.001**	**0.902**
	Right near channel—left near channel	−0.642	2.444	0.237	–

*Significant results (after controlling the False Detection Rate (FDR)) are shown in bold.
[a]'CI' stands for 'confidence interval'.

scores is not expected. We suggest that a combination of our measurement and patients' self-report provides better information to the clinicians. In particular, our method is most useful when in various conditions subjects cannot provide reliable self-report, such as the elderly with dementia and impaired cognition, very young children, or critically ill patients.[29] We hope that our objective measurement provides complimentary information to the self-report for the clinicians.

Undoubtedly, there is a critical need for a reproducible, brief and simple measurement that can correlate subjective pain experience to objective and quantitative parameters for both clinical and research purposes. Reliable biomarkers of pain can help in evidence-based, personalized management of pain. In the present research, we showed that the evoked hemodynamic response to noxious cold water stimuli can be measured using a non-invasive, portable device. Further refinement of the utilized method in this study may enable the measurement of the hemodynamic response at the cortex and the extracranial tissues. These refinements include incorporating advanced signal processing techniques and using other noxious stimuli that would evoke a less generalized systemic response such as hot plates and pressure algometry. Then, fNIRS can be used as a powerful clinical technique to assist clinicians in the assessment of pain with or without subjective self-reports.

ACKNOWLEDGMENTS

We would like to thank Mr. Frank Kepic for his invaluable technical support and advice. Authors also acknowledge Mr. Troy Carlson for designing and constructing the system for cold pressor tests.

REFERENCES

[1]Ayaz, H., P. A. Shewokis, A. Curtin, and M. Izzetoglu. Using MazeSuite and functional near infrared spectroscopy to study learning in spatial navigation. *J. Vis. Exp.* *56*(e3443). doi:10.3791/3443, 2011.
[2]Bartocci, M., L. L. Bergqvist, H. Lagercrantz, and K. Anand. Pain activates cortical areas in the preterm newborn brain. *Pain* 122:109–117, 2006.
[3]Becerra, L., W. Harris, M. Grant, E. George, D. Boas, and D. Borsook. Diffuse optical tomography activation in the somatosensory cortex: specific activation by painful vs. non-painful thermal stimuli. *PLoS One* 4(11):e8016, 2009.
[4]Becerra, L., W. Harris, D. Joseph, T. Huppert, D. A. Boas, and D. Borsook. Diffuse optical tomography of pain and tactile stimulation: activation in cortical sensory and emotional systems. *NeuroImage* 41:252–259, 2008.
[5]Benjamini, Y., and Y. Hochberg. Controlling the false rate discovery: a practical and powerful approach to multiple testing. *J. R. Stat. Soc. B* 57(1):289–300, 1995.
[6]Bland, J. M., and D. G. Altman. Calculating correlation coefficients with repeated observations: part 1—correlation within subjects. *BMJ* 310(6977):446, 1995.
[7]Boynton, G. M., S. A. Engel, G. H. Glover, and D. J. Heeger. Linear systems analysis of functional magnetic resonance imaging in human V1. *J. Neurosci.* 16(13):4207–4221, 1991.
[8]Bozkurt, A., A. Rosen, H. Rosen, and B. Onaral. A portable near infrared spectroscopy system for bedside monitoring of newborn brain. *Biomed. Eng. Online* 4(1):29, 2005. doi: 10.1186/1475-925X-4-29.
[9]Bozkurt, A., and B. Onaral. Safety assessment of near infrared light emitting diodes for diffuse optical measurements. *Biomed. Eng. Online*. 3(9), 2004. doi: 10.1186/1475-925X-3-9.
[10]Buckner, R. L. Event-related fMRI and the hemodynamic response. *Hum. Brain Mapp.* 6:373–377, 1998.
[11]Bunce, S. C., M. Izzetoglu, K. Izzetoglu, B. Onaral, and K. Pourrezaei. Functional near-infrared spectroscopy an emerging neuroimaging modality. *IEEE Eng. Med. Biol.* 25(4):54–62, 2006.
[12]Casey, K. L., S. Minoshima, T. J. Morrow, and R. A. Koeppe. Comparison of human cerebral activation

patterns during cutaneous warmth, heat pain, and deep cold pain. *J. Neurophysiol* 76(1):571–581, 1996.
[13]Chance, B., E. Anday, S. Nioka, S. Zhou, L. Hong, K. Worden, C. Li, T. Murray, Y. Ovetsky, D. Pidikiti, and R. Thomas. A novel method for fast imaging of brain function, non-invasively, with light. *Opt. Express* 2(10): 411–423, 1998.
[14]Cope, M., D. T. Delpy, E. O. Reynolds, J. Wray, and P. van der Zee. Methods of quantitating cerebral near infrared spectroscopy data. *Adv. Exp. Med. Biol*. 222:183–189, 1988.
[15]Dehghani, H., and D. T. Delpy. Near-infrared spectroscopy of the adult head: effect of scattering and absorbing obstructions in the cerebrospinal fluid layer on light distribution in the tissue. *Appl. Opt*. 39(25):4721–4729, 2000.
[16]Devaraj, A. Signal Processing for Functional Near Infrared Neuroimaging. Master's Thesis, Drexel University. 2005.
[17]Di Piero, V., S. Ferracuti, U. Sabatini, P. Pantano, G. Cruccu, and G. L. Lenzi. A cerebral blood flow study on tonic pain activation in man. *Pain* 56:167–173, 1994.
[18]Downie, W. W., P. A. Leatham, V. M. Rhind, V. Wright, J. A. Branco, and J. A. Anderson. Studies with pain rating scales. *Ann. Rheum. Dis*. 37:378–381, 1978.
[19]Gélinas, C., M. Choinière, M. Ranger, A. Denault, A. Deschamps, and C. Johnston. Toward a new approach for the detection of pain in adult patients undergoing cardiac surgery: near-infrared spectroscopy—a pilot study. *Heart Lung* 39(6):485–493, 2010.
[20]Grothusen, J. R., and R. J. Schwartzman. Laser Doppler imaging: usefulness in chronic pain medicine. *Pain Phys*. 15(5):491–498, 2011.
[21]Hines, E. A., and G. E. Brown. A standard stimulus for measuring vasomotor reactions: its application in the study of hypertension. *Mayo Clin. Proc*. 7:332–335, 1932.
[22]Izzetoglu, M., K. Izzetoglu, S. C. Bunce, H. Ayaz, A. Devaraj, B. Onaral, and K. Pourrezaei. Functional near-infrared neuroimaging. *IEEE Trans. Neural Syst. Rehabil. Eng*. 13(2):153–159, 2005.
[23]Lovallo, W. The cold pressor test and autonomic function: a review and integration. *Psychophysiology* 12(3):268–282, 1975.
[24]Music, M., Z. Finderle, and K. Cankar. Cold perception and cutaneous microvascular response to local cooling at different cooling temperatures. *Microvasc. Res*. 81:319–324, 2011.
[25]Okada, E., M. Firbank, M. Schweiger, S. R. Arridge, M. Cope, and D. T. Delpy. Theoretical and experimental investigation of near-infrared light propagation in a model of the adult head. *Appl. Opt*. 36(1):21–31, 1997.
[26]Oldfield, R. The assessment and analysis of handedness: the Edinburgh inventory. *Neuropsychologia* 9(1):97–113, 1971.
[27]Panerai, R. B., S. L. Dawson, P. J. Eames, and J. F. Potter. Cerebral blood flow velocity response to induced and spontaneous sudden changes in arterial blood pressure. *Am. J. Physiol. Heart Circ. Physiol* 280:H2162–H2174, 2001.
[28]Ramsay, J. O., G. Hooker, and S. Graves. Functional Data Analysis with R and MATLAB. Springer, 2009.
[29]Ranger, M., and C. Gélinas. Innovating in pain assessment of the critically ill: exploring cerebral near-infrared spectroscopy as a bedside approach. *Pain Manag. Nurs*. doi:http://dx.doi.org/10.1016/j.pmn.2012.03.005.
[30]Roatta, S., G. Micieli, D. Bosone, G. Losano, R. Bini, A. Cavallini, and P. Magda. Effect of generalised sympathetic activation by cold pressor test on cerebral haemodynamics in healthy humans. *J. Auton. Nerv. Syst*. 71:159–166, 1998.
[31]Rolfe, P. In vivo near infrared spectroscopy. *Annu. Rev. Biomed. Eng*. 2:715–754, 2000.
[32]Saager, R., and A. Berger. Measurement of layer-like hemodynamic trends in scalp and cortex: implications for physiological baseline suppression in functional near-infrared spectroscopy. *J. Biomed. Opt*. 13(3):034017-1–034017-10, 2008.
[33]Seifalian, A. M., G. Stansby, A. Jackson, K. Howell, and G. Hamilton. Comparison of laser Doppler perfusion imaging, laser Doppler flowmetry, and thermographic imaging for assessment of blood flow in human skin. *Eur. J. Vasc. Surg*. 8(1):65–69, 1994.
[34]Sevick, E. M., C. L. Burch, and B. Chance. Near-infrared optical imaging of tissue phantoms with measurement in the change of optical path lengths. *Adv. Exp. Med. Biol*. 345:815–823, 1994.
[35]Stancak, Jr., A., A. Yamamotova, I. P. Kulis, and I. V. Sekyra. Cardiovascular adjustments and pain during repeated cold pressor test. *Clin. Auton. Res*. 6:83–89, 1996.
[36]Streff, A., L. K. Kuehl, G. Michaux, and F. Anton. Differential physiological effects during tonic painful hand immersion tests using hot and ice water. *Eur. J. Pain* 14:266–272, 2010.
[37]Swain, I. D., and L. J. Grant. Methods of measuring skin blood flow. *Phys. Med. Biol* 34(2):151–175, 1989.
[38]Tanida, M., K. Sakatani, R. Takano, and K. Tagai. Relation between asymmetry of prefrontal cortex activities and the autonomic nervous system during a mental arithmetic task: near infrared spectroscopy study. *Neurosci. Lett*. 369:69–74, 2004.
[39]Villringer, A., and B. Chance. Non-invasive optical spectroscopy and imaging of human brain function. *Trends Neurosci*. 20:435–442, 1997.
[40]von Baeyer, C. L., T. Piira, C. T. Chambers, M. Trapanotto, and L. K. Zeltzer. Guidelines for the cold pressor task as an experimental pain stimulus for use with children. *J. Pain* 6(4):218–227, 2005.
[41]Walsh, N. E., L. Schoenfeld, S. Ramamurthy, and J. Hoffman. Normative model for cold pressor test. *Am. J. Phys. Med*. 68(1):6–11, 1989.
[42]Washington, L. L., S. J. Gibson, and R. D. Helme. Age-related differences in the endogenous analgesic response to repeated cold water immersion in human volunteers. *Pain* 89:89–96, 2000.
[43]Watanabe, Y., H. Tanaka, I. Dan, K. Sakurai, K. Kimoto, R. Takashima, and K. Hirata. Monitoring cortical hemodynamic changes after sumatriptan injection during migraine attack by near-infrared spectroscopy. *Neurosci. Res. (Shannon, Irel)* 69:60–66, 2011.
[44]Wolf, S., and J. D. Hardy. Studies on pain. Observations on pain due to local cooling and on factors involved in the "cold pressor" effect. *J. Clin. Invest*. 20(5):521–533, 1941.